Proc. Natl. Acad. Sci. USA
Vol. 82, pp. 7840–7844, December 1985
Biochemistry

Transition-state stabilization in the mechanism of tyrosyl-tRNA synthetase revealed by protein engineering

(enzymology/site-directed mutagenesis)

ROBIN J. LEATHERBARROW†, ALAN R. FERSHT†, AND GREG WINTER‡

†Department of Chemistry, Imperial College of Science and Technology, South Kensington, London SW7 2AY, United Kingdom; and ‡Medical Research Council Laboratory of Molecular Biology, Medical Research Centre, Hills Rd., Cambridge CB2 2QH, United Kingdom

Communicated by William P. Jencks, July 19, 1985

ABSTRACT **The principal catalytic factor in the activation of tyrosine by the tyrosyl-tRNA synthetase is found to be improved binding of ATP in the transition state. The activation reaction involves the attack of the tyrosyl carboxylate on the α-phosphate group of ATP to generate a pentacoordinate transition state. Model building of this complex located a binding site for the γ-phosphate group of ATP, consisting of hydrogen bonds with the side chains of Thr-40 and His-45. Removal of these groups by protein engineering shows that they contribute no binding energy with unreacted ATP but put all of their binding energy into stabilizing the [tyrosine·ATP] transition state [the mutant tyrosyl-tRNA synthetase(Thr-40 → Ala-40; His-45 → Gly-45) has the rate of formation of tyrosyl adenylate lowered by 3.2×10^5 but K_S for ATP is lowered by only a factor of 5]. The side chains of these residues also provide a binding site for pyrophosphate in the reverse reaction. Thus, catalysis is accomplished by stabilization of the transition state by improved binding of a group on the substrate that is distant from the seat of reaction.**

Aminoacyl-tRNA synthetases are responsible for the coupling of an amino acid to its tRNA. For the tyrosyl-tRNA synthetase, as for the majority of aminoacyl-tRNA synthetases, aminoacylation of tRNA proceeds by a two-step process: (*i*) the amino acid is activated by the formation of an enzyme-bound aminoacyl adenylate (Eq. 1) and (*ii*) there is transfer to tRNA (Eq. 2) (1) (where E = enzyme).

$$E + \text{tyrosine} + ATP \rightarrow E\cdot Tyr\text{–}AMP + PP_i \quad [1]$$

$$E\cdot Tyr\text{–}AMP + tRNA^{Tyr} \rightarrow E + Tyr\text{-}tRNA^{Tyr} + AMP \quad [2]$$

The mechanisms whereby these processes are catalyzed are completely unknown.

The structure of the tyrosyl-tRNA synthetase from *Bacillus stearothermophilus* has been determined to 0.21-nm resolution, and the locations of enzyme-bound tyrosine and tyrosyl adenylate are known (2). The enzyme is a dimer of 2 × 47 kDa. In the crystal structure, however, only the NH_2-terminal 320 amino acids (out of 419) give well-resolved structure in the electron-density map. These residues account fully for the activation reaction, whereas the 99 residues of the COOH terminus are essential for tRNA binding and hence transfer (3). Catalysis and specificity in the tyrosyl-tRNA synthetase from *B. stearothermophilus* have been investigated recently by systematic application of site-directed mutagenesis (4–6).

The amino acid residues of tyrosyl-tRNA synthetase that interact with the bound tyrosyl adenylate are known from the crystallographic studies, but there is no immediate indication of how they catalyze the reaction. The chemical mechanism of the reaction, as shown in Fig. 1, involves the simple attack of the carboxylate group of tyrosine on the α-phosphate group of ATP, resulting in the elimination of magnesium pyrophosphate (7). The classical enzymatic processes of acid–base or covalent catalysis would not seem to be applicable to this reaction as it consists of the attack of a fully ionized good nucleophile on an activated compound with a good leaving group (the magnesium pyrophosphate from ATP).

In this study, we use model building of the probable transition state in the reaction pathway to implicate catalytic interactions with the enzyme. We know the structure of the enzyme-bound tyrosyl adenylate complex, and so we are able to build the transition state for the formation of tyrosyl adenylate by the addition of pyrophosphate to its α-phosphate moiety. To test our predictions, we use site-directed mutagenesis to replace the residues implicated. Kinetic analysis of mutant enzymes then allows quantitation of the interactions involved.

MATERIALS AND METHODS

Construction of Mutant Proteins. The following oligonucleotide primers were synthesized to direct the mutations. Thr-40 → Ala-40: 5′ CCGCCGC*CGGGTCAAAC 3′ (* = mismatched base); His-45 → Gly-45: 5′ GGCCGATAC*C*CAAACTGT 3′. Site-directed mutagenesis was performed on the tyrosyl-tRNA synthetase gene cloned in the vector M13 mp93 (5, 8). The double-mutant tyrosyl-tRNA synthetase(Thr-40 → Ala-40; His-45 → Gly-45) was constructed by using the His-45 → Gly-45 primer to mutate the tyrosyl-tRNA synthetase(Thr-40 → Ala-40) gene. Mutant enzymes were purified as described by Lowe *et al.* for other mutants (9). All were electrophoretically homogeneous and formed 1 mol of tyrosyl adenylate per mol of enzyme.

Kinetic Procedures. The kinetic constants for the formation of tyrosyl adenylate by tyrosyl-tRNA synthetase were determined in all cases from presteady-state kinetics by direct observation of the formation of enzyme-bound tyrosyl adenylate. Tyrosyl-tRNA synthetase(His-45 → Gly-45) was studied by stopped-flow fluorescence over a period of 0–5 min (10). For tyrosyl-tRNA synthetase(Thr-40 → Ala-40) and tyrosyl-tRNA synthetase(Thr-40 → Ala-40; His-45 → Gly-45), the rate constant for tyrosyl adenylate formation was sufficiently low to allow a single turnover of the enzyme to be followed by manual sampling. The amount of enzyme-bound tyrosyl adenylate was determined at various time intervals by nitrocellulose disc assay [active-site titration (11)]. For tyrosyl-tRNA synthetase(Thr-40 → Ala-40), a complete time course was monitored and the rate constant was determined at various substrate concentrations from the best-fit first-order exponential to the data. For tyrosyl-tRNA synthetase(Thr-40 → Ala-40; His-45 → Gly-45), the rate constant was determined from the initial rate of the reaction (0–15% completion) and the known enzyme concentration. Michaelis–

The publication costs of this article were defrayed in part by page charge payment. This article must therefore be hereby marked "*advertisement*" in accordance with 18 U.S.C. §1734 solely to indicate this fact.

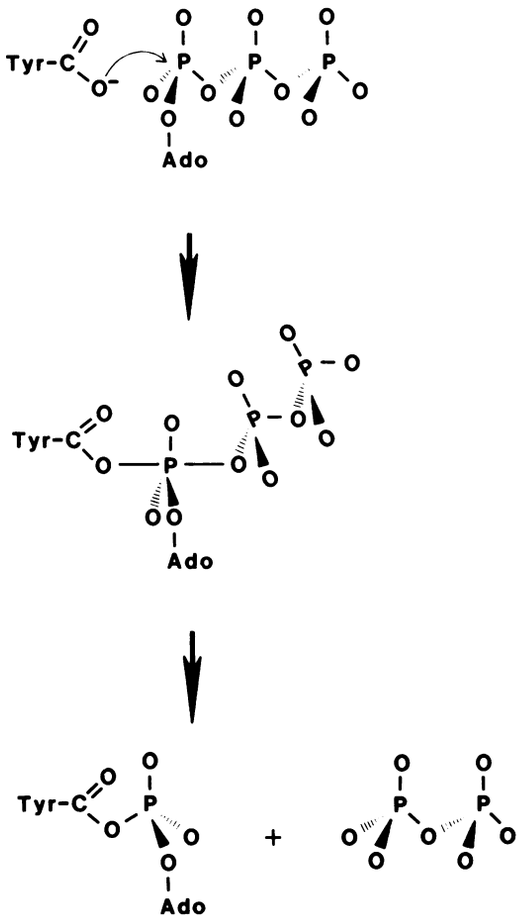

FIG. 1. Chemical mechanism of formation of tyrosyl adenylate from tyrosine and ATP.

Menten kinetics were followed by all of the enzymes studied. Values for k_3 and K_S were calculated from the variation of rate constant with substrate concentration. The rates of pyrophosphorolysis of the enzyme-bound tyrosyl adenylates were monitored by nitrocellulose disc filtration on the addition of pyrophosphate to preformed samples of enzyme-bound tyrosyl adenylate. When studying the effect of Mg^{2+} ions, solutions were pretreated, by batchwise adsorption, with Chelex 100 (Bio-Rad).

Computer Graphics. Model building was performed by using the program FRODO using coordinates kindly supplied by P. Brick and D. M. Blow.

RESULTS

Model Building of Reaction Intermediates. Chemical studies have shown that formation of tyrosyl adenylate from tyrosine and ATP results in inversion at the α-phosphorus (7). Since no covalent enzyme-bound intermediates occur, it is implied that the mechanism involves an "in-line" displacement, with the tyrosyl carboxylate acting as a nucleophile and the pyrophosphate being the leaving group (Fig. 1). Such a reaction scheme implies a pentacoordinate transition state. Since enzymic catalysis must involve interactions with the transition state, we adopted the following strategy to delineate the amino acid residues involved. First, starting from the crystallographic structure of the enzyme-bound tyrosyl adenylate, we utilized computer graphics to construct a model of the transition state using a P—O axial bond length of 0.24 nm (12). Finally, by allowing bond rotations around the O—P bonds we looked for interactions with the enzyme that could be implicated in the catalytic mechanism.

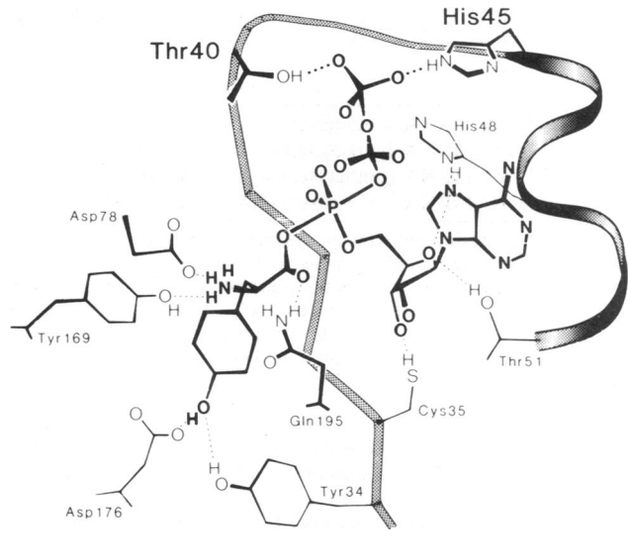

FIG. 2. Model building of the pentacoordinate transition state of the reaction into the crystallographic structure of the tyrosyl-tRNA synthetase. The transition state structure was extrapolated from the known structure of enzyme-bound tyrosyl adenylate. Interactions are shown between the γ-phosphate and the side chains of Thr-40 and His-45.

From the model building we found that the γ-phosphate group of the intermediate could be placed to interact with the side chains of Thr-40 and His-45 (Fig. 2). These side chains are positioned so that each can make similar polar interactions via the β-OH and NϵH groups, respectively. We should note that His-45 is conserved between various amino acyl-tRNA synthetases (ref. 13; unpublished data), implying an important role for this residue. Although Mg^{2+} is required for the reaction, for simplicity we have not built a Mg^{2+} ion into this model. There is sufficient space for Mg^{2+} to interact with the phosphate groups on the opposite face to that presented to Thr-40/His-45, and we present evidence below that mutation of Thr-40 and His-45 does not affect the binding of magnesium.

Site-Directed Mutagenesis. Although model building suggests a role for the Thr-40 and His-45 side chains, confirmation and quantitation of their involvement require more direct evidence. To provide this, site-directed mutagenesis was used to remove the interacting side chains. The following mutants were constructed and their kinetics were analyzed according to Scheme 1, which fits the data for catalysis by tyrosyl-tRNA synthetase and all of its mutants. In this scheme, k_{-pp} is found to be fast compared with k_{-3}, and k_{cat} equals k_3 in the presteady state (unpublished data). The second kinetic parameter, K_M, is equal to the substrate dissociation constant, K_S, in the presteady state (i.e., equals k'_t/k'_{-t} or k'_a/k'_{-a} for tyrosine and ATP, respectively).

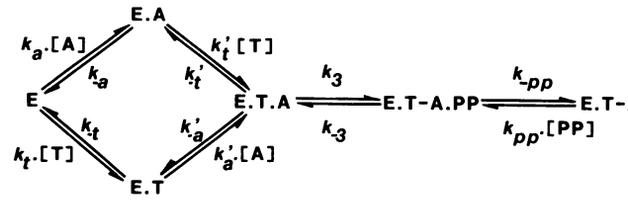

SCHEME 1

Tyrosyl-tRNA Synthetase(Thr-40 → Ala-40). In this mutation, the -OH group of the threonine is replaced by an H,

Table 1. Presteady state kinetic parameters for formation of tyrosyl adenylate

Enzyme	k_3,* s^{-1}	K_S for tyrosine, μM	K_S for ATP, mM
Tyrosyl-tRNA synthetase†	38	12	4.7
Tyrosyl-tRNA synthetase(His-45 → Gly-45)	0.16	10	1.2
Tyrosyl-tRNA synthetase(Thr-40 → Ala-40)	0.0055	8.0	3.8
Tyrosyl-tRNA synthetase(Thr-40 → Ala-40; His-45 → Gly-45)	0.00012	4.5	1.1

Experiments were performed at 25°C at pH 7.8 (144 mM Tris·HCl) in the presence of 10 mM $MgCl_2$ (free), 1 unit of inorganic pyrophosphatase per ml, 14 mM 2-mercaptoethanol, and 0.1 mM phenylmethylsulfonyl fluoride under presteady state conditions. k_3 is the forward rate constant for the formation of tyrosyl adenylate (Scheme 1); K_S is the dissociation constant for the substrate ($= k'_{-t}/k'_t$ or k'_{-a}/k'_a for tyrosine and ATP, respectively).

*Extrapolated to infinite substrate concentrations.

†From Wells and Fersht (14). The value of K_S for tyrosine of wild-type enzyme was obtained from equilibrium dialysis and equals k_{-t}/k_t.

removing any hydrogen bonding interaction between residue 40 and the γ-phosphate group of the transition state. The rate constant for formation of tyrosyl adenylate, k_3, by the Ala-40 enzyme is found to be >3 orders of magnitude lower than the native enzyme, whereas values of K_S are hardly altered (Table 1). The time course for a single turnover of the enzyme could be followed by nitrocellulose disc assay over 30–60 min (Fig. 3). In the reverse reaction the rate constant k_{-3} for wild-type enzyme is 14 s^{-1} and K_{pp} ($= k_{-pp}/k_{pp}$) is 0.7 mM (10). For this mutant, k_{-3}/K_{pp} is 3.6 $s^{-1}\cdot M^{-1}$ and K_{pp} is raised to >8 mM. (Measurements are limited by the solubility of magnesium pyrophosphate.)

Tyrosyl-tRNA synthetase(His-45 → Gly-45). This mutation removes the interacting imidazole side chain. The rate constant for this mutant enzyme is again much less than that of the native enzyme, although it is somewhat higher than for the previous mutant. K_S for tyrosine is unaffected and K_S for ATP is lowered by a factor of 4 (Table 1).

Tyrosyl-tRNA synthetase(Thr-40 → Ala-40; His-45 → Gly-45). As expected, the rate constant for tyrosyl adenylate formation for the double mutant is considerably lower than for either of the previous mutants. The time required for formation of 1 mol of bound tyrosyl adenylate per mol of enzyme is ≈6–8 hr under conditions of saturating concentrations of substrates and is much longer for subsaturating concentrations. The kinetic parameters were therefore obtained from the initial rates of reaction (0–15% completion), monitored by nitrocellulose filter assays over a period of 45 min. k_3 is reduced by 3.2×10^5 but values of K_S for ATP and tyrosine are lowered by factors of only 3–4 (Table 1). In the reverse reaction, k_{-3}/K_{pp} is 0.11 $s^{-1}\cdot M^{-1}$ and K_{pp} is >20 mM.

It should be noted that the rate constants for the activation of tyrosine by the mutants tyrosyl-tRNA synthetase(Thr-40 → Ala-40) and tyrosyl-tRNA synthetase(Thr-40 → Ala-40; His-45 → Gly-45) are so low that they could not be reliably measured by steady-state kinetics. Not only would the rate be difficult to detect but there could be complications that the observed rate may be due to contaminating enzymes or even small amounts of wild-type enzyme generated by infidelities in protein synthesis (misincorporation of amino acids occurs at levels of 10^{-4}–10^{-3}). The measurement of rate constants was possible because presteady-state kinetics was used to detect the rate of formation of 1 mol of tyrosyl adenylate per mol of enzyme. The accumulation of tyrosyl adenylate was in turn allowed because the mutations Thr-40 → Ala-40 and His-45 → Gly-45 reduced only the rate of reaction and not the binding constants of substrates and tyrosyl adenylate.

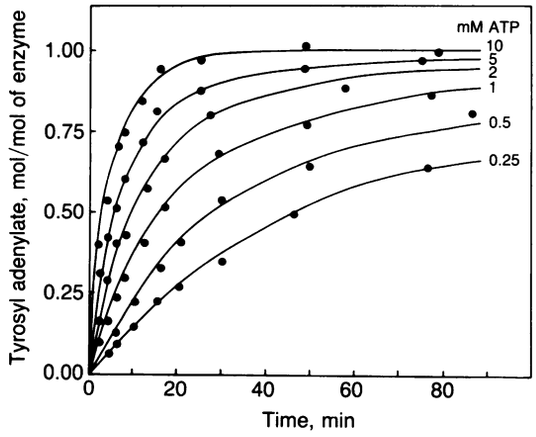

FIG. 3. Time course of formation of enzyme-bound tyrosyl adenylate by tyrosyl-tRNA synthetase(Thr-40 → Ala-40) with varying concentrations of ATP. The concentration of tyrosine was 30 μM.

Effect of Mg^{2+}. It is unlikely that the results of these mutations arise from a change in the Mg^{2+} requirements for the reaction. Removal of magnesium from the reaction mixtures reduces the activity of wild-type enzyme by a factor of $>10^3$ and abolishes activity of the mutants. Doubling or halving the Mg^{2+} concentration has no effect on the rates of the mutant enzymes, showing that the dissociation constant has not been raised to a high level (results not shown).

DISCUSSION

Mutations at positions 40 and 45 of the tyrosyl-tRNA synthetase have little effect on the dissociation constants of tyrosine, ATP, and tyrosyl adenylate from the enzyme. The binding of pyrophosphate, however, is severely weakened. The most striking feature is the large reduction of the rate constant k_3. Because of the lack of effect on the binding of both substrates and enzyme-bound products, it is unlikely that there is any serious structural change in the enzyme on mutation of these residues. Instead, it is indicated that there is a weakening of binding of pyrophosphate in both the transition state and E·Tyr–AMP·PP complexes. Our model building suggests that Thr-40 and His-45 can form a binding site for the γ-phosphate group of ATP in the transition state and for pyrophosphate in the reverse reaction. The kinetic data show that this binding site contributes no net binding energy for ATP in the enzyme–substrate complex.

Mutation of the γ-phosphate binding site (Thr-40 → Ala-40; His-45 → Gly-45) results in an increase in the energy level of the transition state complex, whereas the energy levels of the enzyme–substrate complex are unaltered (Fig. 4). This results in increased activation energy and consequently lowered k_3. Therefore, these kinetic studies provide direct evidence for stabilization of the transition state as a major factor in the catalytic mechanism of this enzyme.

Magnitude of Catalysis. The tyrosyl-tRNA synthetase has binding sites for tyrosine and ATP that locate the substrates in the correct orientation for reaction. In this way, it converts the nucleophilic attack from an entropically unfavorable

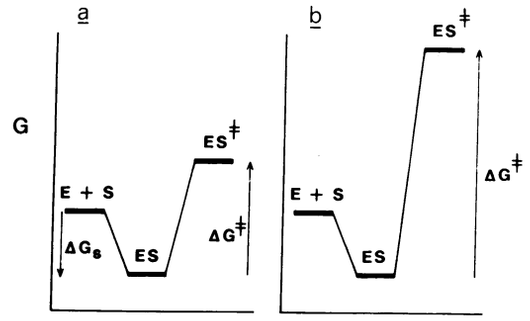

FIG. 4. Schematic Gibbs energy changes for the formation of tyrosyl adenylate by (*i*) tyrosyl-tRNA synthetase and (*ii*) mutant enzymes that have greatly reduced values of k_3 but unaltered K_S. The reaction is E + S $\rightleftharpoons$ ES $\xrightarrow{k_3}$ products, where E = enzyme, S = substrate, and ES = enzyme-bound transition state. K_S is proportional to ΔG_S; k_3 is proportional to $\Delta G^{\ddagger}$ (15). The effect of the mutation is to raise the energy level of the transition state of the reaction.

second-order reaction in solution to a first-order reaction with a concomitant rate enhancement (16). A simple model for the reaction between a carboxylate and a phosphate ester in an enzyme–substrate complex is the cyclization of 2-carboxyphenyl *p*-nitrophenylphosphate (Eq. 3) (17).

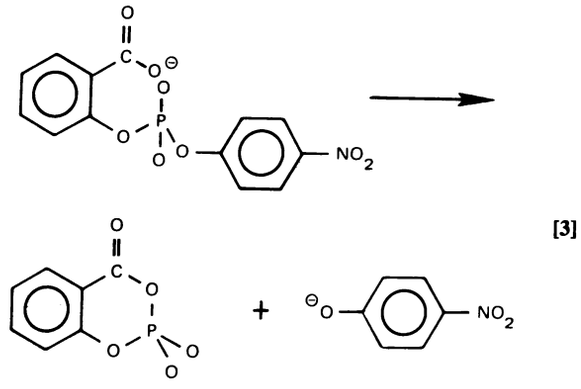

[3]

p-Nitrophenol is an equivalent leaving group to magnesium pyrophosphate because both have similar pK_a values of around 7. The intramolecular cyclization is very rapid compared with its bimolecular counterpart because of the favorable entropy (16) (although there are also possible effects of strain in this compound). The effective concentration of the carboxyl group is estimated to be 6×10^8 M (18), at the upper extreme suggested by Page and Jencks (16). We estimate from the published data at 39°C allowing for a lower pK_a of tyrosine [pK_a of 2 compared with 4 in the model compound (17)] that the equivalent uncatalyzed rate between bound tyrosine and ATP would be *ca.* 10^{-3} s^{-1} at 25°C. This is within the same order of magnitude as that of our least reactive mutant and suggests that the reaction with this enzyme is little more than a simple intramolecular reaction. The wild-type enzyme has a turnover number of 38 s^{-1}, some 4×10^4 times faster than the solution model. Thus, a further factor of 10^4–10^5 or so is required to raise the rate of "uncatalyzed" enzymic reaction, and the transition state stabilization clearly can account for a large fraction of this.

How Does the Enzyme Use the Binding Energies of Thr-40 and His-45 to Stabilize the Transition State and Not the Unreacted Substrate? One possibility, as in Fig. 5, is that the enzyme takes advantage of the large change in bond angles about the α-phosphate group as it goes from four- to five-

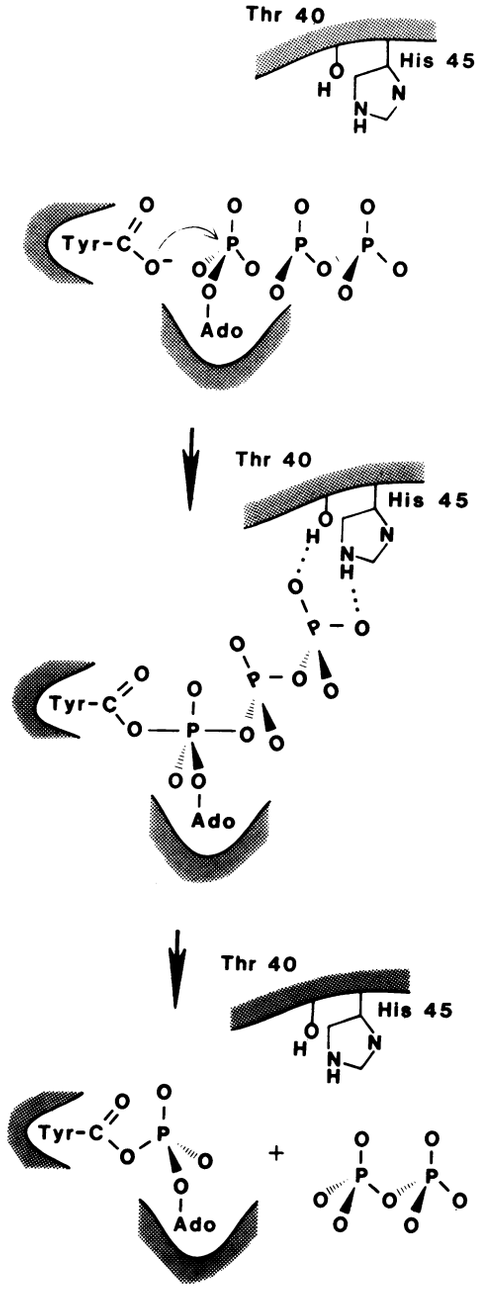

FIG. 5. Schematic mechanism for the catalysis of tyrosyl adenylate formation by tyrosyl-tRNA synthetase. Interactions are made by the side chains of Thr-40 and His-45 to the γ-phosphate group of the transition state.

coordinate. It is possible that the γ-phosphate of substrate ATP does not bind between Thr-40 and His-45 but just remains solvated by water. During the reaction, it swings into its binding site and releases the solvated water. Preliminary data on the activation energies of wild-type and tyrosyl-tRNA synthetase(Thr-40 → Ala-40) support this model because both enzymes have similar enthalpies of activation, but the wild-type enzyme has a more positive entropy of activation (unpublished data). Direct structural evidence on the location of bound ATP would help resolve the mechanistic possibilities. Unfortunately, it has so far proved impossible to solve the crystal structure of the enzyme–ATP complex by x-ray diffraction because of the poor binding (19).

We therefore suggest that the formation of tyrosyl adenylate proceeds by the following mechanism (Fig. 5). (*i*) By

providing suitable binding sites for tyrosine and ATP, the enzyme brings the reactive groups together. In this way, binding energy is used to offset the loss of entropy on two molecules coming together (16). (*ii*) By locating the side chains of Thr-40 and His-45 in suitable positions to stabilize the transition state, the enzyme greatly enhances the rate of reaction—loss of these interactions in the tyrosyl-tRNA synthetase(Thr-40 → Ala-40; His-45 → Gly-45) reduces the rate by a factor of >300,000. In this way, binding energy is used to increase catalytic rate.

Use of Binding Energy to Increase Catalytic Rate. It is important to note that interactions made by Thr-40 and His-45 at the γ-phosphate group are distant from the seat of reaction at the α-phosphate. The extent of the rate enhancement provided illustrates dramatically how enzymes can utilize binding energy to increase the rate of chemical catalysis. This concept was originally suggested in 1930 by Haldane, who proposed that appropriate binding sites on an enzyme may be used to help pull apart or push together substrates (20), and was elaborated by Pauling, who proposed that an enzyme should be complementary to, and thus bind preferentially, the transition state rather than the substrate (21). Theoretical considerations (15, 22, 23) show that the rate of reaction is optimized when binding interactions are favored in the enzyme-transition state over the enzyme–substrate complex. This improved binding energy lowers the activation energy of the reaction, increasing the rate. In the tyrosyl-tRNA synthetase, our results show that the side chains of Thr-40 and His-45 make substantially better interactions with the Tyr·ATP transition state than with the enzyme–substrate complex. In addition to the large effects of positions 40 and 45, it has been found that hydrogen bonding groups even further removed from the seat of reaction can cause smaller, but still significant, rate enhancements by preferential binding of the transition state (14).

Previous evidence for transition-state stabilization in enzyme catalysis has come somewhat indirectly from the binding of transition state analogues, from model building, and from kinetic studies on substrate series (23). By the use of protein engineering, we not only provide direct evidence for this type of mechanism in tyrosyl-tRNA synthetase but also identify the groups involved and quantitate the energetics of their involvement.

1. Fersht, A. R. & Jakes, R. (1975) *Biochemistry* **14,** 3350–3356.
2. Blow, D. M. & Brick, P. (1985) in *Biological Macromolecules and Assemblies: Nucleic Acids and Interactive Proteins*, eds. Jurnak, F. & McPherson, A. (Wiley, New York), Vol. 2, pp. 442–469.
3. Waye, M. M. Y., Winter, G., Wilkinson, A. J. & Fersht, A. R. (1983) *EMBO J.* **2,** 1827–1829.
4. Fersht, A. R., Shi, J.-P., Knill-Jones, J., Lowe, D. M., Wilkinson, A. J., Blow, D. M., Brick, P., Carter, P., Waye, M. M. Y. & Winter, G. (1985) *Nature (London)* **314,** 235–238.
5. Winter, G., Fersht, A. R., Wilkinson, A. J., Zoller, M. & Smith, M. (1982) *Nature (London)* **299,** 756–758.
6. Fersht, A. R., Shi, J.-P., Wilkinson, A. J., Blow, D. M., Carter, P., Waye, M. M. Y. & Winter, G. (1984) *Angew. Chem.* **23,** 467–473.
7. Lowe, G. & Tansley, G. (1984) *Tetrahedron Lett.* **40,** 113–117.
8. Carter, P. J., Winter, G., Wilkinson, A. J. & Fersht, A. R. (1984) *Cell* **38,** 835–840.
9. Lowe, D. M., Fersht, A. R., Wilkinson, A. J., Carter, P. & Winter, G. (1985) *Biochemistry* **24,** 5106–5109.
10. Fersht, A. R., Mulvey, R. S. & Koch, G. L. E. (1975) *Biochemistry* **14,** 13–18.
11. Wilkinson, A. J., Fersht, A. R., Blow, D. M. & Winter, G. (1983) *Biochemistry* **22,** 3581–3586.
12. Boyd, D. B. (1969) *J. Am. Chem. Soc.* **91,** 1200–1205.
13. Barker, D. G. & Winter, G. (1982) *FEBS Lett.* **145,** 191–193.
14. Wells, T. N. C. & Fersht, A. R. (1985) *Nature (London)* **316,** 656–657.
15. Jencks, W. P. (1975) *Adv. Enzymol.* **43,** 219–410.
16. Page, M. I. & Jencks, W. P. (1971) *Proc. Natl. Acad. Sci. USA* **68,** 1678–1683.
17. Khan, S. A., Kirby, A. J., Wakselman, M., Horning, D. P. & Lawler, J. M. (1970) *J. Chem. Soc. (B)*, 1182–1187.
18. Kirby, A. J. (1980) *Prog. Phys. Org. Chem.* **17,** 183.
19. Monteilhet, C., Blow, D. M. & Brick, P. (1984) *J. Mol. Biol.* **173,** 477–485.
20. Haldane, J. B. S. (1930) *Enzymes* (Longmans, Green, London).
21. Pauling, L. (1946) *Chem. Eng. News.* **24,** 1375.
22. Fersht, A. R. (1974) *Proc. R. Soc. London Ser. B* **187,** 397–407.
23. Fersht, A. R. (1985) *Enzyme Structure and Mechanism* (Freeman, New York), pp. 311–346.